

A new method for the evaluation of the accuracy of full-arch digital impressions in vitro

Jan-Frederik Güth¹ · Daniel Edelhoff¹ · Josef Schweiger¹ · Christine Keul¹

Received: 6 July 2015 / Accepted: 1 October 2015 / Published online: 10 October 2015
© Springer-Verlag Berlin Heidelberg 2015

Abstract

Objectives Introducing a new approach to evaluate the accuracy of digital impression methods for full-arch scans, avoiding “best-fit alignment.”

Materials and methods A lower jaw model with a straight metal bar between the second molars of both quadrants was directly digitized using an intraoral scanner (True Definition, TRD, $n=12$) and indirectly digitized (D810, CON, $n=12$) after impression and plaster cast. A dataset of the bar from a coordinate measuring machine served as reference (REF). Datasets obtained from test groups were analyzed using inspection software to determine the aberration of the bar length, the linear shift (in X -, Y -, Z -axis) and the angle deviation (α_{overall} , α_{coronal} , $\alpha_{\text{horizontal}}$) caused by the digitalization method. Mann–Whitney U and unpaired two-sample Student’s t test were implemented to detect differences. The level of significance was set at 5 %.

Results Concerning the bar length, no significant differences were found between groups. In view of the linear shift, CON showed significantly higher values than TRD in Y -axis ($p=0.003$) and in Z -axis ($p=0.040$). Regarding the angle measurement, TRD showed significant smaller values than CON for α_{overall} ($p=0.006$) and for α_{coronal} ($p=0.005$).

Conclusions This in vitro study shows that intraoral scanning systems seem to show the same or even higher accuracy than the conventional impression with subsequent indirect digitalization.

Clinical relevance Intraoral scanners have proven excellent accuracy for single teeth or small spans. However, insufficient data is available about their accuracy for full-arch scans. The presented new approach seems to be suitable to precisely analyze differences in the accuracy of different digitalization methods without using best-fit alignment.

Keywords Full-arch scan · Digital impression · Intraoral scanner · Accuracy · CAD/CAM · Digital workflow

Introduction

The digital workflow for dental restorations by computer-aided design and computer-aided manufacturing (CAD/CAM) was successfully introduced in dental treatment concepts over the last decades. The initial step of the CAD/CAM workflow is the generation of a three-dimensional virtual replica of the clinical situation, thus the digitalization [1]. This commencing step is followed by the designing (CAD) and manufacturing (CAM) of the prosthetic restoration [1]. The main advantage of this CAD/CAM fabrication process is its standardization and reproducibility paired with a high cost efficiency and superior quality [2, 3]. This means that the digitalization process directly influences the adaptation and the fit of dental restorations, which is again a decisive factor for their longevity [3].

By means of direct (chairside) and indirect (labside) digitalization, two options to access the digital workflow are currently available [4]. The indirect digitalization, based on a conventional impression and/or plaster casts that are digitized in the dental laboratory, represents today’s most common method [4, 5]. This again means that the basis of the highly accurate digital manufacturing process is still a conventional impression that involves several potential sources of error

✉ Jan-Frederik Güth
jan_frederik.gueth@med.uni-muenchen.de

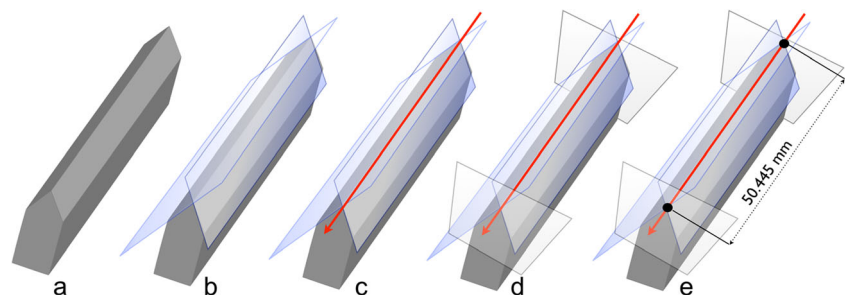
¹ Department of Prosthodontics, Dental School of the Ludwig-Maximilians University Munich, Goethestraße 70, 80336 Munich, Germany

biasing the final outcome [6–11]. To obtain more predictable treatment outcomes and fit of restorations, it is necessary to avoid the common errors caused by conventional impressions.

Against this background, the direct data capturing in the oral cavity, using an intraoral scanner, seems to be the logical access to the digital workflow. However, one fundamental requirement for the application of intraoral scanners is their comparable or superior accuracy to the conventional way. Regarding the digitalization from single teeth through to a quadrant, most intraoral scanning devices seem to offer a sufficient accuracy and data quality to compete with indirect digitalization [6, 7, 12, 13]. At the present point in time, there are contradictory results regarding the scans of complete arches. Some data are available that direct digitalization showed similar accuracy for in vitro tests to that of the conventional impression [14]. Also in comparison to a special reference scanning system, the majority of tested intraoral scanners resulted in a comparable level of accuracy for full-arch scanning [15]. Conversely, another study showed that digital impressions were significantly less accurate than conventional impressions [4]. Compared to the intraoral scanning procedure, the extraoral scanning with a laboratory device resulted in higher accuracy [16]. It could be shown that by using the adequate scanning strategy, highly accurate full-arch dental impressions can be produced with intraoral scanning systems [17]. Literature shows that the available accuracy is already sufficient for orthodontic analysis and treatments [18], whereas the scanning of multiple implants over a full arch seems to be very limited [19, 20].

Nevertheless, most studies analyzing full arches with teeth used a best-fit algorithm for superimposition of virtual datasets previous to the analysis of differences. Therefore, the results might be influenced by the quality of superimposition and the interpretation of differences. Therefore, the purpose of the present study was to introduce an innovative approach and method to evaluation of the accuracy of intraoral scanning devices without the application of a best-fit alignment. In this study, a new device for direct digitalization (True Definition Scanner) was evaluated in comparison with the well-established indirect digitalization method, using a standardized metal bar within one jaw as an appropriate reference structure. The null hypothesis was that no quantitative accuracy differences will occur between direct and indirect digitalization methods.

Fig. 1 Measurement of the CMM data of the straight bar using Geomagic Qualify inspection software



Material and methods

The study was based on a polyurethane mandible model (AlphaDie MF, LOT 2012008441; Schütz Dental GmbH, Rosbach, Germany) in which an straight metal bar (GARANT, DIN 875-00-g; Hoffmann Group, Munich, Germany) was inserted to connect both quadrants in the region of 37 and 47.

Reference measurement of the bar

To determine reference values of the bar surface, it was measured using a coordinate measuring machine (CMM: Mitutoyo Crysta Apex C 574; Createch Medical, Mendaro, Spain; software: MCOSMOS Mitutoyo Software; Mitutoyo, Neuss, Germany) at a temperature of 20 °C before placing it in the model. The measurements were made to the following specifications: MPEe 1.9 microns + (3*L/1000) where *L* is the real length of the bar.

The resulting surface tessellation language (STL) data was imported into inspection software (Geomagic Qualify 13.0.2.1219; Geomagic, Morrisville, NC, USA). Four planes were constructed by marking the surface on the bar by using the “contact feature mode” of the inspection software:

- Anterior plane of the bar (APB)
- Posterior plane of the bar (PPB)
- Vestibular plane of the bar third quadrant (VPB3)
- Vestibular plane of the bar fourth quadrant (VPB4)

The intersection of APB and PPB leads to one intersection line on the edge of the bar (vector VB). The intersection of the vector VB with VPB3 and VPB4 resulted in the points PB3 and PB4, respectively. To determine the length of the bar as a reference (*R*), the distance between PB3 and PB4 was calculated and amounted to *R*=50.445 mm (Fig. 1).

Scanning of the full-arch model

After CMM measurement, the full-arch mandibular model, including the straight bar, was reproduced by two methods simulating the conventional clinical workflow (CON) and intraoral scanning (TRD).

For group CON, conventional monophasic impressions with a polyether material (Impregum Penta, LOT 514064; 3M ESPE, Seefeld, Germany; $n=12$) were taken of the polymeric full-arch model, including the bar, in line with the manufacturer's recommendations. Therefore, light-cured custom-made trays (Palatray XL, LOT 132651; Heraeus Kulzer, Hanau, Germany) to ensure optimal material thickness were used. The impressions were made at constant room temperature of 20 °C to avoid any expansion of the metal bar and the model. According to clinical procedures, the impressions were stored for 2 min in a disinfection bath (ORBI-sept Abformdesinfektion, LOT A0984; Orbis Dental Handelsgesellschaft mbH, Münster, Germany). For manufacturing of the casts, the impressions were stored in an air-conditioned laboratory (20°; humidity between 40–60 %) for 24 h and then poured with a type IV—plaster (Resin Rock, LOT 041071308; Whip Mix Corporation, Louisville, KY, USA) using scan powder (BlueSpray, LOT A0181; Dreve Dentamid GmbH, Unna, Germany). The indirect digitalization with a laboratory scanner (D810, Dental Manager 2013–1; 3shape, Copenhagen, Denmark, distributed by BEGO GmbH & Co. KG, Bremen, Germany with an open STL interface) was carried out at the earliest 48 h after casting, and STL data were exported (CON 1–12).

For group TRD, the polymeric full-arch model, including the bar, was scanned with an intraoral scanner (True Definition Scanner, Scanning Software 4.0.3.1; 3M ESPE, Seefeld, Germany/ $n=12$). Therefore, the model and the bar were lightly dusted with titanium oxide powder (LAVA Scanpowder; 3M Espe, Seefeld, Germany). Hereby, a stochastic pattern was generated on the model surface, as a prerequisite for accurate scanning. After the powder application, the homogeneity and quality of the powder layer was scrutinized using the “video mode” of the device. The powder layer was removed by steam and renewed before each of the 12 scans. Scanning was conducted applying a specific scanning procedure: starting in the fourth quadrant on tooth 48 holding the wand in sagittal direction. After alignment with the jaw, the tooth row was scanned from occlusal, vestibular, and oral using a “zick-zack movement” until region 31. Then, the wand was moved back over tooth 44 and was horizontally turned 180°. Scanning was completed in the third quadrant using the same movement patterns. After this first scan, the result was saved and a second scan was conducted in the opposing direction using the same strategy. Without saving the second scan, the procedure was completed by capturing approximately 1.5 mm of each end of the metal bar. However, it was of special interest that the opposing ends of the bar were not connected in the virtual dataset. The scanning time was between 5:20 and 5:45 min per scan, including the scan of the bar ends (about 30 s each). The datasets were sent online to the “research lab” and corresponding STL datasets (TRD 1–12) were exported. The scanning strategy is displayed in Fig. 2.

Three-dimensional analysis of datasets

For analysis, all STL datasets (CON 1–12; TRD 1–12) were imported into Geomagic Qualify software and aligned with the coordinate system in the same direction: XY-plane represented the coronal plane, whereas the Z-axis points in sagittal direction. Therefore, the occlusal (horizontal) plane was represented by the XZ-plane (Fig. 3).

Each dataset was analyzed individually using the same constructed and fitted geometric objects (features), applying the following procedure

In both quadrants, three planes were constructed by marking the surface on the bar segments respectively. As displayed in Fig. 3, the following planes were created using the “contact feature mode” of the inspection software. This mode was applied to ensure that the constructed virtual geometrical planes only touched the outer surfaces of the test datasets, instead of penetrating through them.

- Third quadrant
 - Anterior plane third quadrant (AP3)
 - Posterior plane third quadrant (PP3)
 - Vestibular plane third quadrant (VP3)
- Fourth quadrant
 - Anterior plane fourth quadrant (AP4)
 - Posterior plane fourth quadrant (PP4)
 - Vestibular plane fourth quadrant (VP4)

From the intersections of the anterior and posterior planes, one vector resulted for each quadrant (third quadrant: V3; fourth quadrant: V4). Further on, the intersection of the vector V3 with plane VP3 and the vector V4 with the plane VP4 defined the points P3 and P4, respectively.

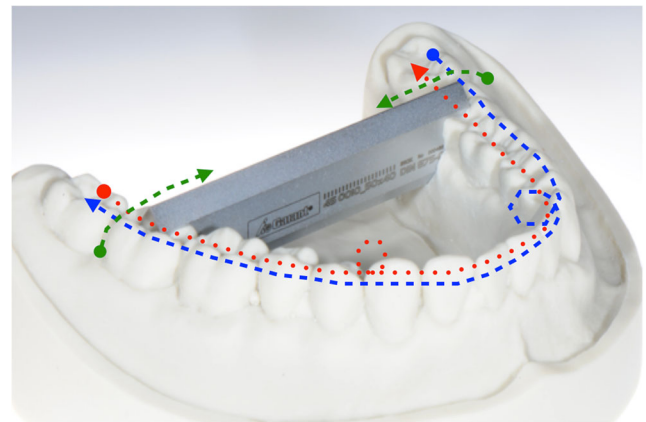
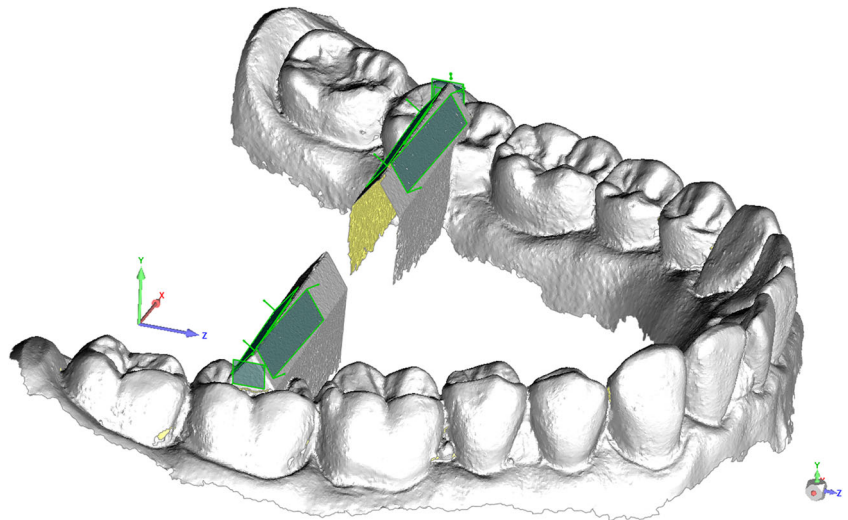


Fig. 2 Scanning strategy using the True Definition Scanner

Fig. 3 Dataset standardized aligned with the coordinate system (XY-plane represents the coronal plane, whereas the Z-axis points in sagittal direction). The constructed “contact features” are displayed in green color



Evaluation of bar length

The length of the bar in the three-dimensional datasets (L) was measured between point P3 and point P4. Therefore, the x -, y -, and z -coordinates of both points were imported into Microsoft Excel 2010 (Microsoft Corporation, Redmond, WA), and L was calculated using the Euclidean formula to transfer coordinates into distances:

$$L = \sqrt{(x_{P4} - x_{P3})^2 + (y_{P4} - y_{P3})^2 + (z_{P4} - z_{P3})^2}$$

where L is the length of the bar and x , y , and z are the x -, y -, and z -coordinates of P3 and P4.

The difference value (ΔL) to the reference bar length (R) was calculated by

$$\Delta L = L - R$$

Evaluation of linear shift in X-, Y-, and Z-axis

For the evaluation of the linear shift, the plane VP3 was parallel shifted by 50.4452 mm (CMM length of the bar) in the direction of the fourth quadrant, resulting in plane VP3'. Then, point P3' was constructed by the intersection of the vector V3 with plane VP3'. The vectorial error (\vec{V}_E) was then calculated between point P3' and P4 to receive the linear shift in millimeter on X-, Y-, and Z-axis using the following formula:

$$\vec{V}_E = \begin{pmatrix} x_{P4} - x_{P3'} \\ y_{P4} - y_{P3'} \\ z_{P4} - z_{P3'} \end{pmatrix}$$

where x , y , and z are the x -, y -, and z -coordinates of P3' and P4.

Evaluation of angle measurement

For the evaluation of the angles in different directions, initially the overall angle (α_{overall}) between V3 and V4 was calculated using the formula

$$\alpha_{\text{overall}} = \alpha \cos \frac{x_{V3} \cdot x_{V4} + y_{V3} \cdot y_{V4} + z_{V3} \cdot z_{V4}}{\sqrt{x_{V3}^2 + y_{V3}^2 + z_{V3}^2} \cdot \sqrt{x_{V4}^2 + y_{V4}^2 + z_{V4}^2}} \cdot \frac{180}{\pi}$$

where x , y , and z are directions of the vectors V3 and V4 in X-, Y-, and Z-axis.

To distinguish the rotation in coronal and horizontal direction, α_{overall} was mathematically projected on the XY-plane (α_{coronal}) and the XZ-plane ($\alpha_{\text{horizontal}}$) using the following formulas

$$\alpha_{\text{coronal}} = \alpha \cos \frac{x_{V3} \cdot x_{V4} + y_{V3} \cdot y_{V4}}{\sqrt{x_{V3}^2 + y_{V3}^2} \cdot \sqrt{x_{V4}^2 + y_{V4}^2}} \cdot \frac{180}{\pi}$$

$$\alpha_{\text{horizontal}} = \alpha \cos \frac{x_{V3} \cdot x_{V4} + z_{V3} \cdot z_{V4}}{\sqrt{x_{V3}^2 + z_{V3}^2} \cdot \sqrt{x_{V4}^2 + z_{V4}^2}} \cdot \frac{180}{\pi}$$

where x , y , and z are the directions of the vectors V3 and V4 in X-, Y-, and Z-axis

Evaluation of reproducibility

Previous to the study itself, pilot tests were carried out in which one dataset was analyzed 12 times using the described method. For the bar length, results varied within 1 μm . Also, the measurement of the overall angle showed a high reproducibility with an alteration within 0.002°, when the same dataset was analyzed 12 times.

Statistics

For all parameters, descriptive statistics (mean, standard deviation, median, and 95 % confidence intervals) were calculated. Normality of data distribution was tested using Shapiro–Wilk test. Unpaired two-sample Student’s *t* test (for mean) combined with Levene test (homogeneity of variances) was applied for groups that showed normal data distribution. Mann–Whitney *U* test was applied in case the groups showed no normal distribution. For data analysis, the Statistical Package for the Social Science Version 20 (SPSS Inc., Chicago, USA) was used. The level of significance was set at 5 % ($p < 0.05$).

Results

Table 1 gives the descriptive statistics of all measured parameters of CON and TRD.

Evaluation of bar length

Shapiro–Wilk test revealed a normal distribution for bar length values. Therefore, the mean values were compared with an unpaired Student’s *t* test. The mean value of group CON differed not significantly from group TRD ($p = 0.499$). In all 24 datasets, positive values (datasets stretched in transversal direction) could be found. Figure 4 depicts the values of the single measurements together with a trend line.

Evaluation of linear shift in X-, Y-, and Z-axis

Shapiro–Wilk test revealed a normal distribution for the deviation in X-, Y-, and Z-axis. Therefore, the mean values were compared with an unpaired Student’s *t* test. For the deviation in X-axis, the mean value of group CON and that of group TRD showed no significant difference ($p = 0.084$). Regarding the deviation in Y-axis, CON showed significantly higher values than TRD ($p = 0.003$). Likewise, in Z-axis, values for CON were significantly higher than TRD ($p = 0.040$).

Evaluation of angle measurement

For the parameters α_{overall} , α_{coronal} , and $\alpha_{\text{horizontal}}$, Shapiro–Wilk test showed no normal distribution of data within the test groups. Therefore, Mann–Whitney *U* test was applied for statistical comparison. Group TRD showed for α_{overall} significant smaller angles than group CON ($p = 0.006$). Also for α_{coronal} group, TRD showed significant smaller values than group CON ($p = 0.005$). No significant difference was found between CON and TRD ($p = 0.060$) for $\alpha_{\text{horizontal}}$.

Discussion

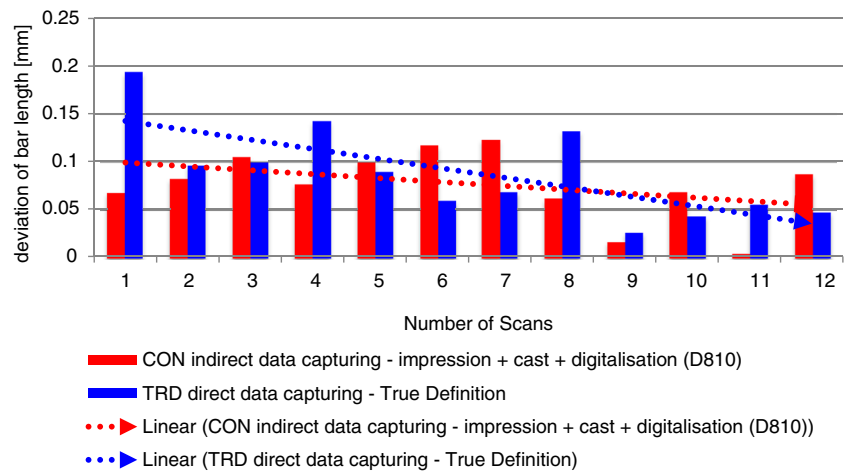
The presented study introduces a new approach for the evaluation of the accuracy of conventional and digital impressions of complete arches that differs fundamentally from previous published methods. Considering the results, the hypothesis—that no quantitative accuracy differences will occur between direct and indirect digitalization methods—has to be partially rejected. Linear deviations in Y- and Z-axis, as well as the overall angle measurements and the angle in coronal direction, differed significantly between the groups. For the bar length, the linear deviation in X-axis, and the angle in horizontal direction, no significant differences could be observed.

Previous studies mostly applied best-fit algorithms to superimpose test datasets from different impression methods with one accurate reference dataset [14, 15, 21]. Hereby, point-to-point spatial differences between the surfaces of the digital models were measured using the signed nearest neighbor method [14, 15, 21]. For scans right up to one quadrant, the method of best-fit seems to be suitable, because the error caused by the superimposition itself between test and reference dataset is within an acceptable range [6, 7, 12]. However, the larger the datasets are and the more they differ under each other, the bigger the influence of the error becomes, caused by the process of superimposition. Therefore, the aim of this study was to introduce a method that avoids any dataset superimposition. Another advantage of the new approach is that

Table 1 Descriptive statistics with mean values (M), standard deviation (SD), median (MED), and 95 % confidence interval (CI) of both groups

		CON indirect data capturing impression + cast + digitalization (D810)				TRD direct data capturing True Definition			
		M	SD	MED	CI	M	SD	MED	CI
Deviation bar length between test and reference dataset [mm]		0.077	0.036	0.080	0.053/0.100	0.089	0.048	0.080	0.057/0.120
Linear shift [mm]	X-axis	0.068	0.037	0.071	0.042/0.092	0.099	0.048	0.088	0.067/0.130
	Y-axis	0.154	0.304	0.174	−0.037/0.348	−0.185	0.064	−0.184	−0.226/−0.145
	Z-axis	0.042	0.076	0.024	−0.006/0.091	−0.027	0.078	−0.028	−0.076/0.023
Angle measurement [°]	α_{overall}	1.347	1.700	0.915	0.266/2.427	0.293	0.126	0.264	0.212/0.373
	α_{coronal}	0.150	2.049	−0.433	−1.152/1.452	0.270	0.119	0.236	0.194/0.346
	$\alpha_{\text{horizontal}}$	−0.378	0.700	−0.152	−0.822/0.067	0.003	0.125	0.034	−0.076/0.083

Fig. 4 Single values of bar length measurement of both investigated methods with trend lines



a highly accurate CMM measurement of a geometrical object can serve as reference for the accuracy. Additionally, the bias of the measurement method could be minimized, by analyzing the reference dataset from CMM and the test datasets using the same measurement strategy. Further on, the presented method without need of a best-fit algorithm allows to measure real numerical values for linear shifts in all three dimensions as well as for the evaluation of angles. This allows a clear statement regarding the three-dimensional directions of inaccuracies in X -, Y -, and Z -axis. Regardless, whether a best-fit algorithm is applied or real measurements are conducted, the terms “trueness” and “precision” are appropriate to describe the accuracy of results [22].

However, based on the above facts, it is difficult to compare the measured values with the available literature. It can be assumed that the different methods and approaches may lead to controversial results regarding the accuracy of different impression techniques for full arches. On the basis of a metal reference model (cobalt–chromium alloy) of an upper jaw, conventional and digital impressions resulted in similar values for trueness (conventional impression $55 \pm 21.8 \mu\text{m}$, LAVA C.O.S. $40.3 \pm 14.1 \mu\text{m}$, CEREC Bluecam $49 \pm 14.2 \mu\text{m}$) and precision (conventional impression $61.3 \pm 17.9 \mu\text{m}$, LAVA C.O.S. $60.1 \pm 31.3 \mu\text{m}$, CEREC Bluecam $30.9 \pm 7.1 \mu\text{m}$) [14]. Opposed to this, another study on the basis of the same evaluation methodology stated that conventional impressions showed significantly higher precision ($12.5 \pm 2.5 \mu\text{m}$) and trueness ($20.4 \pm 2.2 \mu\text{m}$) values, while digital impressions were significantly less accurate with a precision of $32.4 \pm 9.6 \mu\text{m}$ and a trueness of $58.6 \pm 15.8 \mu\text{m}$ [4]. One investigation of different systems for digital impressions showed a trueness ranging from 38.0 to 332.9 μm and precision values from 37.9 to 99.1 μm depending on the intraoral scanning system [15]. However, hereby no comparison to the conventional impression technique was investigated. Also, the interpretation and computing mode of the differences after best-fit evaluation differs within studies concerning the accuracy of impression methods.

Prior investigations used plaster casts with fitted PEEK cylinder [23] or metal-based [4, 14, 24] models as reference. Generally, plaster casts confer the benefit of non-reflective surfaces compared to metal ones. However, mechanical stress and/or humidity changes between the single impressions may induce an alteration of the surface [15]. Also, it seems to be inconceivable to perform a series of conventional impressions using elastomers on a plaster reference model without damaging the surface. Opposing to this, a metal-based reference model demonstrates a constant stability with lower susceptibility against outside influences. However, the reflective properties may bias the performance of intraoral scanning systems. This requires a prior treatment by powder application or a matting of the surface for example by airborne-particle abrasion [24]. The applied bar model combines the good scanable surface of a polyurethane model with the high accuracy of a metal reference object. Due to the “active wavefront sampling”—operating technology of the True Definition, a stochastic powder pattern is required on the surface prior to scanning. To guarantee stable dimensions of the reference bar, all impressions were performed under constant controlled room temperature within 1 day.

In the current study, the length of the bar did not significantly differ between both impression methods. This means that the horizontal dimension is within the same range for both investigated digitalization methods. Noteworthy is that all datasets were stretched horizontally and no dataset showed a “compression” of the bar. However, the conventional impression shows a significantly higher overall angle. This might be explainable by the deformation occurring during the tray removal after impression and the recovery of the impression material that might not be compensated completely. The recovery potential of polyether is dependent on the setting time and arises with it [25]. Observed scattered outliers for specific specimens might also be explainable by a detachment of the impression material from the tray that could not be detected by the operator. Also clinically, this is a relevant factor that can be easily overlooked, during the visual assessment of the impression, and that negatively affects the fit of

the resulting restoration. Especially when capturing full arches, a mean overall angle of about 1.3° might cause severe misfits of splinted restorations on the abutments, as well as influences the occlusal relation. Even more severe are the clinical consequences in implant-supported splinted restorations due to rigid osseointegration [26]. This was confirmed by Gimenez et al., testing different optical scanning systems on a multi-implant model [19, 20, 27]. Especially, digitalization of multiple angulated implants seems to lead to diminished accuracy [27].

The accuracy of the three-dimensional dataset is dependent on the correct scanning protocol [17]. Therefore, it was stated that full-arch dental impressions result in a high accuracy, if adequate scan strategies are used. Before performing the present study, the operator who performed all digital impressions was specially trained in using the correct scanning protocol given in the **Material and methods** section. The in vitro testing environment offered ideal premises to follow the scanning protocol accurately and to scan in optimal focus distance. As a limitation of the study, it has to be questioned, if the scanning strategy used can be also applied under clinical conditions. Also, the performance of different intraoral scanning systems is, limited by the presence of saliva, blood, or subgingival margins, dependent on the scanning technology. For the present study, a laboratory design on basis of an in vitro model was selected to facilitate standardized ideal conditions for the assessment of data. Compared with this, for performing in vivo tests, the influence of blood or saliva, the lack of space, or infra-gingival preparation margins cannot completely be ruled and are different between single individuals. Also, the individual influence of patients with the presence of saliva, blood, or movements may result in a noticeable effect on the accuracy. Therefore, the authors are currently planning to adapt the developed method for in vivo tests.

The results of the present study provide evidence that the digital impression using the True Definition intraoral scanner offers the potential to achieve comparable or even higher accuracy compared to the conventional impression method. The results highlight the tendency toward the high potential of digital impression techniques.

Conclusions

Within the limitations of the current in vitro study, it can be concluded:

- The presented approach using a straight bar measurement seems to be a reliable method to analyze deviations in full-arch datasets after conventional and digital impressions.
- The intraoral scanner True Definition showed significantly lower values for the linear shift in Y- and Z-axis, as well as for the overall angle and the angle in coronal direction than the conventional impression technique followed by indirect digitalization.

Acknowledgments The authors thank 3M ESPE, Seefeld, Germany, for the support of the study and Createch medical, Mendaro, Spain, for conducting the CMM measurements.

Compliance with ethical standards The present study does not contain clinical patient data.

Conflict of interest The study was supported by a research grant from 3M Espe Company (Seefeld, Germany). The first and second authors declare that they receive personal fees from 3M ESPE, Seefeld, Germany, outside the submitted work for scientific lectures.

References

1. Beuer F, Schweiger J, Edelhoff D (2008) Digital dentistry: an overview of recent developments for CAD/CAM generated restorations. *Br Dent J* 204:505–511
2. Miyazaki T, Hotta Y, Kunii J, Kuriyama S, Tamaki Y (2009) A review of dental CAD/CAM: current status and future perspectives from 20 years of experience. *Dent Mater J* 28:44–56
3. Bosch G, Ender A, Mehl A (2014) A 3-dimensional accuracy analysis of chairside CAD/CAM milling processes. *J Prosthet Dent* 112: 1425–31
4. Ender A, Mehl A (2013) Accuracy of complete-arch dental impressions: a new method of measuring trueness and precision. *J Prosthet Dent* 109:121–128
5. Quaas S, Rudolph H, Luthardt RG (2007) Direct mechanical data acquisition of dental impressions for the manufacturing of CAD/CAM restorations. *J Dent* 35:903–908
6. Guth JF, Keul C, Stimmelmayer M, Beuer F, Edelhoff D (2013) Accuracy of digital models obtained by direct and indirect data capturing. *Clin Oral Investig* 17:1201–1208
7. Keul C, Stawarczyk B, Erdelt KJ, Beuer F, Edelhoff D, Guth JF (2014) Fit of 4-unit FDPs made of zirconia and CoCr-alloy after chairside and labside digitalization—a laboratory study. *Dent Mater* 30:400–407
8. Christensen GJ (2008) The challenge to conventional impressions. *J Am Dent Assoc* 139:347–349
9. Christensen GJ (2008) Will digital impressions eliminate the current problems with conventional impressions? *J Am Dent Assoc* 139:761–763
10. Chandran DT, Jagger DC, Jagger RG, Barbour ME (2010) Two- and three-dimensional accuracy of dental impression materials: effects of storage time and moisture contamination. *Biomed Mater Eng* 20:243–249
11. Al-Bakri IA, Hussey D, Al-Omari WM (2007) The dimensional accuracy of four impression techniques with the use of addition silicone impression materials. *J Clin Dent* 18:29–33
12. Mehl A, Ender A, Mormann W, Attin T (2009) Accuracy testing of a new intraoral 3D camera. *Int J Comput Dent* 12:11–28
13. Boeddinghaus M, Breloer ES, Rehmann P, Wostmann B (2015) Accuracy of single-tooth restorations based on intraoral digital and conventional impressions in patients. *Clin Oral Investig*. doi: 10.1007/s00784-015-1430-7
14. Ender A, Mehl A (2011) Full arch scans: conventional versus digital impressions—an in-vitro study. *Int J Comput Dent* 14:11–21
15. Patzelt SB, Emmanouilidi A, Stampf S, Strub JR, Att W (2014) Accuracy of full-arch scans using intraoral scanners. *Clin Oral Investig* 18:1687–1694
16. Flugge TV, Schlager S, Nelson K, Nahles S, Metzger MC (2013) Precision of intraoral digital dental impressions with iTero and

- extraoral digitization with the iTero and a model scanner. *Am J Orthod Dentofac Orthop* 144:471–478
17. Ender A, Mehl A (2013) Influence of scanning strategies on the accuracy of digital intraoral scanning systems. *Int J Comput Dent* 16:11–21
 18. Grünheid T, McCarthy SD, Larson BE (2014) Clinical use of a direct chairside oral scanner: an assessment of accuracy, time, and patient acceptance. *Am J Orthod Dentofac Orthop* 146:673–82
 19. Giménez B, Özcan M, Martínez-Rus F, Pradies G (2015) Accuracy of a digital impression system based on active triangulation technology with blue light for implants: effect of clinically relevant parameters. *Implant Dent* 24:498–504
 20. Giménez B, Pradies G, Martínez-Rus F, Özcan M (2015) Accuracy of two digital implant impression systems based on confocal microscopy with variations in customized software and clinical parameters. *Int J Oral Maxillofac Implants* 30:56–64
 21. Ender A, Mehl A (2015) In-vitro evaluation of the accuracy of conventional and digital methods of obtaining full-arch dental impressions. *Quintessence Int* 46:9–17
 22. Accuracy (trueness and precision) of measurement methods and results—part 1: general principles and definitions (ISO 5725–1:1994)
 23. van der Meer WJ, Andriessen FS, Wismeijer D, Ren Y (2012) Application of intra-oral dental scanners in the digital workflow of implantology. *PLoS One* 7, e43312
 24. Seelbach P, Brueckel C, Wostmann B (2013) Accuracy of digital and conventional impression techniques and workflow. *Clin Oral Investig* 17:1759–1764
 25. Balkenhol M, Haunschild S, Erbe C, Wöstmann B (2010) Influence of prolonged setting time on permanent deformation of elastomeric impression materials. *J Prosthet Dent* 103:288–294
 26. Sahin S, Cehreli MC (2001) The significance of passive framework fit in implant prosthodontics: current status. *Implant Dent* 10:85–92
 27. Giménez B, Özcan M, Martínez-Rus F, Pradies G (2015) Accuracy of a digital impression system based on active wavefront sampling technology for implants considering operator experience, implant angulation, and depth. *Clin Implant Dent Relat Res* 17(1):e54–64